energies

Article

A long-term wind speed ensemble forecasting system with weather adapted correction

Yiqi Chu [1], Chengcai Li [1,*], Yefang Wang [1,2], Jing Li [1] and Jian Li [1]

[1] Department of Atmospheric and Oceanic Sciences, School of Physics, Peking University, Beijing, 100871, China;

[2] Baicheng Ordnance Test Center of China, Baicheng 137001, China ;

* Correspondence: ccli@pku.edu.cn

Academic Editor: name

Received: date; Accepted: date; Published: date

Abstract: Wind forecasting is critical in the wind power industry, yet forecasting bias often exists. In order to effectively correct the forecasting bias, this study develops a weather adapted bias correction scheme on the basis of an average bias-correction method, which considers the bias of estimated error associated with the difference in weather type within each unit of the statistical sample. This method is tested by an ensemble forecasting system based on the Weather Research & Forecasting Model (WRF). This system outputs high resolution wind speed deterministic forecast at six wind fields located on the east coast of China, using 40 members generated by initial perturbations and multi-physical schemes. The forecast system output 28-52h predictions with a temporal resolution of 15 minutes, and was evaluated against collocated anemometer towers observations. Results show that the information contained in weather types produces an improvement in forecast bias correction.

Keywords: wind power; wind forecasting; statistical correction; weather classification; ensemble forecasting.

1. Introduction

As a kind of clean energy, wind power is receiving increasing attention and application in the world, under the recent concern about energy crisis and global warming issues **[1, 2]**. However, a wind field's output power strongly depends on local real-time wind speed and is thus uncontrollable. The fluctuation of wind speed will inevitably lead to the fluctuation of the output power of the wind farm. As a result, in order to stabilize the voltage in the power grid, the portion of wind power in the regional power grid must be limited to a certain level, namely the wind power penetration limit **[3]**. This penetration limit severely restricts wind power's extensive application.

One solution to this problem is to provide near surface wind speed forecast with a high temporal resolution, from which the prediction of wind fields' output power can be obtained **[4]**. This method has been proven effective in numerous practices **[5]**. However, because of imperfect models and uncertain initial conditions, bias always exists in numerical weather prediction (NWP) output **[6]**. In this case, a statistical correction to NWP is an effective means to reduce prediction bias without the potentially expensive cost to improve the model scheme and initial fields **[7-10]**. There have been a lot of work testing and improving various statistical correction methods in order to improve the forecast skill of NWPs **[1]**. Typical approaches include comparison and combination of different statistical models **[11-14]** and NWP datasets **[15]**, and incorporating more input parameters.

Generally speaking, statistical correction is to construct a statistical model between historical prediction error and single or multiple input parameters, in order to estimate the forecast error at the time to be corrected according to the values of these parameters. However, by using a single parameter, for example, the predicted value is insufficient in limiting the range of error estimation. Therefore, improvements have been made by adding more parameters for better estimation accuracy. Previously, parameters to be added in statistical models mostly focused on day/ night flag **[16]**, the forecast length **[17]** and seasonality, as these parameters are physically related to prediction bias and are able to gain along with the prediction. On the other hand, predictions of other meteorological variables besides the wind speed are often added in models. In some works, researchers have proven that the combination of wind direction and wind speed is effective in reducing the error of prediction **[18, 19]**, temperature and pressure can also improve the performance of statistical models **[20, 21]**. However, in many circumstances, especially under complicated weather conditions, these parameters still cannot offer enough information for bias estimation and sometimes even worsen the forecast results, which implies that some additional or more relevant parameters are needed to provide more complete information.

As a summary of the entire regional meteorological field at a certain moment **[22]**, weather type is clearly related to the meteorological conditions and thus the wind field. This parameter not only contains information of seasons, and day and night, but it also reflects environmental conditions in both the local site and nearby area. In this way, statistical correction models can be equipped with more spatial information compared to those using merely local meteorological factors. While weather classification has been widely used in many fields, such as climate analysis **[23-25]**, wind reconstruction **[26]** and weather prediction **[27, 28]**, it has not been conventionally applied or considered in the wind energy field for forecast bias correction.

In this paper, we defined a variable named weather type based on the classification of the meteorological field, and test its effect in improving long-term wind forecast skill in a business forecasting system. Compared to traditional bias correction methods, this modified scheme considers typical errors of NWP in different weather types, thus the prediction errors of sampling units can be corrected to an expected value in the same weather type as the focus period. We will show that the addition of weather types has a positive effect in long-term wind forecast, and it performed better in ensemble average prediction than non-ensemble prediction due to the higher correlation between prediction errors and weather type.

The paper is organized as follows. Section 2 describes the ensemble forecasting system. Section 3 presents the principle of the correction method. Section 4 shows results and the evaluation. Conclusions and some discussions are given in Section 5.

2. The Ensemble Forecasting System

This section may be divided by subheadings. It should provide a concise and precise description of the experimental results, their interpretation as well as the experimental conclusions that can be drawn.

2.1. Numerical model

This study was based on the Weather Research & Forecasting Model (WRF) **[29]**, which has been well known and widely used in research and practical application. As a meso-scale meteorological model, WRF model is able to predict weather processes with a resolution of kilometers, and simulates sub-scale processes by parameterization. Vertically, WRF model uses eta levels to describe pressure layers depending on local surface pressure.

In this research, a single grid domain was constructed with a horizontal resolution of 18 kilometers. Considering the requirement of near surface prediction, the eta levels in the model were set with an increasing density near surface, with four levels located below 100 meters above the ground. The time step in the simulation was set to be 60 seconds in order to increase the stability of model.

2.2. Ensemble member production

The forecasting system used the Global Forecasting System (GFS) data published by NCEP as the initial field. In subsequent processes, by adding random perturbation into the initial field and using multi-physical schemes, an ensemble containing 40 members was produced.

The multi-scheme is a prediction skill that uses different physical parameters and schemes for different members in ensemble forecasting. In this research, we chose different schemes from 4 physical processes, which produced 40 different combinations. The multi-scheme included 3 microphysics (MP) process schemes [Lin et al. (Lin et al. 1983), WSM 3-class simple ice scheme (Hong et al. 2004), WSM 6-class scheme (Hong et al. 2006)]，4 land surface (SFC) schemes [thermal diffusion scheme (MM5), unified Noah land-surface model (Noah), RUC land-surface model (Smirnova et al. 1997, 2000), Pleim-Xu scheme (Development of a Land Surface Model Pleim & Xiu 2003)]，3 cumulus (CU) schemes [Kain-Fritsch (Kain & Fritsch 1993), Betts-Miller (Betts & Miller 1986; Janjic 1994), Grell-Devenyi (Grell & Devenyi 2002)]，and 2 planet boundary layer (PBL) schemes [YSU (Noh et al. 2006), MYJ (ETA; Janjic 1994)]. Table in Appendix A lists the combination of physical schemes for each ensemble member.

2.3. Forecasting system design

The wind farms chosen in this research are located on the east coast of China. The local observational data comes from anemometer towers in these wind farms, with a 15 minute temporal resolution, in accordance with the requirements of the State Grid Corporation of China. The height of the wind tower is 70m, which is consistent with the hub height of wind turbines.

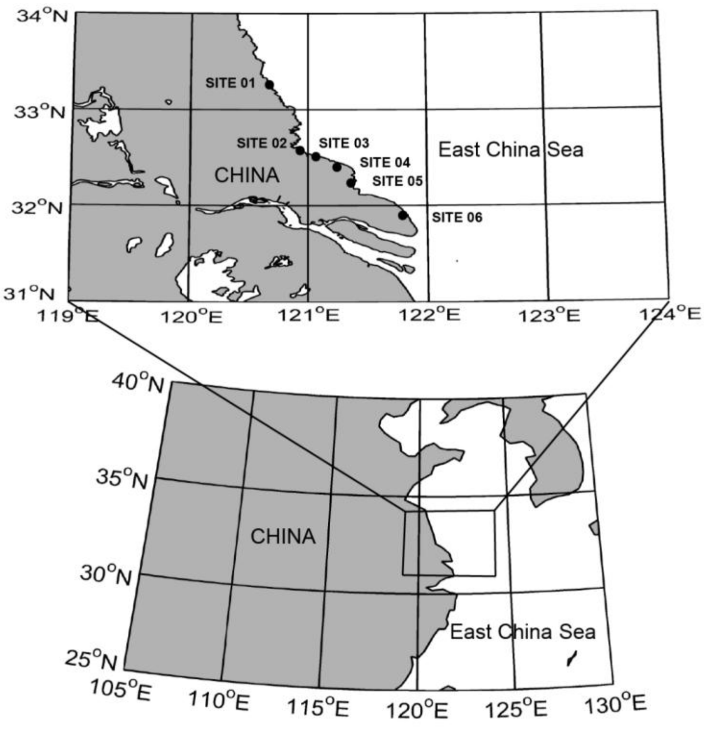

Figure 1. Location of the six wind farms used in this study, denoted by black dots.

The terrain of this area is flat coastal beach. For this reason, the local wind speed has obvious diurnal variation and a fluctuation at a period of several days. Moreover, during the summer season, the local weather may be influenced by typhoons and severe convective weather systems, as well as by front systems with a typical 1-3 day time scale. Therefore the local wind speed has distinct seasonal characteristics.

This research used NCEP FNL (Final) Operational Global Analysis data from 2005 to 2012 to obtain 18 typical weather types, and established a statistical correlation between forecast errors and weather types with ensemble average forecasts from Sep. 2013 to Aug. 2014. Ensemble forecasts from Sep. 2014 to Jan. 2015 were used to test the weather adapted correction method.

According to the requirement of the State Grid Corporation of China, the forecasting system needs to publish the prediction of wind speed of the second day at LST 8:00 am (Beijing, UTC+8). Considering the delay of GFS data's publishing and receiving, and the time cost of simulation, the forecasting system chose the UTC 1200 GFS global field to be the initial field, therefore the output prediction was 28-52h ahead.

Finally the system output field was the ensemble mean of the 40 members. The 70m wind speed of target wind farms were extracted from the output field to be the NWP primary deterministic product, followed by the statistical correction presented below.

3. Statistical correction

In numerical simulation, the bias of prediction comes from two aspects, namely the error of the initial field and the defects of numerical models. Generally speaking, the model error can be divided into systematic error and random error **[30]**. Comparing with random error, the systematic error can be estimated and reduced through statistical methods, by comparing with historical data. This method is called the statistical correction to numerical prediction, through which the prediction error could be reduced, and the forecasting result could be improved. In the fact that the defects of models are unavoidable, it is effective and necessary to develop statistical correction methods, which are based on historical experience, to improve model prediction skill.

The statistical correction methods can be generally divided into two categories **[30]**. The first is posterior correction, which means to make correction to the final output after the numerical integration of the model; the second is to periodically modify the variables along the model integration. In this research, the posterior correction method was applied in the forecasting system.

3.1. Weather classification system

Weather classification is a methodology that summarizes several typical weather types by analyzing specific meteorological variables, and then classifies the meteorology fields into these weather types. As the background fields of local weather propagate, the weather type at larger scales is usually correlated with local weather processes **[22]**. Therefore weather classification can be used for identification and prediction of various weather processes, and helps to improve weather forecast skills.

There are two main approaches to realize weather classification, namely classification of air mass and classification of circulation **[31]**. The air mass classification refers to the classification typically bases on surface variables such as pressure and temperature, which can reflect local weather conditions. On the other hand, circulation classification depends on the field of sea level pressure (SLP), geopotential height, or some other fields that can describe the atmospheric circulation on a regular NWP grid. Compared to air mass classification, the performance of circulation classification is generally superior in that it considers the influence of both large-scale circulation and local meteorological variables **[32]**.

In this research, the European Cooperation in Science and Technology Action 733 (COST733) system **[33]** was applied to weather classification in China. The COST733 system is originally used to achieve a general numerical method for assessing, comparing and classifying weather situations in Europe, and has good performance in previous research **[34-36]**. This system has also been applied to weather classification in areas outside Europe **[34]**, because it has high operability and credibility, and contains plenty of classification schemes.

The clustering algorithm used in this research is t-mode principal component analysis using oblique rotation **[37]**. This method can avoid the "snowball effect" in a certain extent, which means most of the sample units are classified as one same type in calculation, and few sample units in other types **[38]**. This algorithm thus ensures that each type has a relatively comprehensive sample size. The algorithm has been already realized in COST733 **[33]** (methods: PCT), and has been applied in some published researches **[39]**.

Considering that the aims of weather classification is to distinguish the difference between NWP errors of different weather types, the number of weather types should be large enough so that some important samples would not be ignored. On the other hand, weather type number should not be too small, in order to ensure that all the types have enough samples to keep their representative. In the test, 18 different weather types model satisfied these requirement and got applied.

3.2. Combined correction method

The correction method in this research was based on the average bias correction method, a low-cost, widely used method in wind energy prediction. It uses 15 days before the focus day as the statistical sample, equally divides each day into four segments with 6 hours in each, and then calculates the average forecast error for each period. The forecast error for the four segments of the focus day is estimated as the average error in the corresponding historical periods.

In this section, we refined the average bias correction by considering the correlation between prediction error of sample units and corresponding weather types, and attempted to reduce this error when using units with different weather types to estimate the target error.

We used the FNL reanalysis data from 2005 to 2012 to build up the classification model. The FNL data is published 4 times each day with a six-hour interval. Thus it is possible to classify the target wind fields in each 6 hour period, and the statistical sample volume is large enough to support a classification of 18 weather types. In the next step, the ensemble average predictions from Sep. 2013 to Aug. 2014 were classified according to the weather types produced by FNL data. The peak value of prediction error distribution of each weather type was used as the characteristic error of model prediction in this weather type.

In the original correction process, the average error of each sampling unit was used as the final estimation of the target error in this period. While in the refined method, this average error was further corrected according to the difference between characteristic errors of the unit's weather type and the target period's weather type. Then in the accumulation, the updated errors are used to estimate the target error, in the same manner as the original method.

In this way, the prediction error of a sample unit was corrected as an estimation of the forecast error of the units in the same weather type, thus the weather types of both historical units and target unit were consistent.

4. Results

4.1. Weather classification

In order to evaluate the effect of weather classification, we chose ensemble forecast data of 6 costal wind farms during the period from Sep. 2013 to Aug. 2014. We calculated the probability density function (PDF) of prediction error for each weather type.

According to prediction error distributions shown in the figures above, the majority of weather types has a monomodal distribution, although a few have distributions with multiple peaks or no obvious peak. As a result, the distributions are able to reflect the impact of weather types on statistical correction, and the peak value of distribution can be set as the characteristic error.

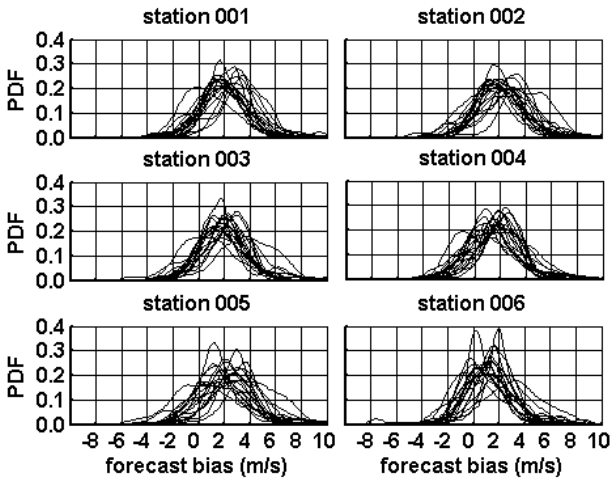

Figure 2. Prediction error distribution of 18 weather types in each of six wind farms.

To further evaluate the classification results, we calculated the average characteristic radius of each weather type cluster and the differentiation degree of the clusters. Here we defined the average characteristic radius rad_i, the differentiation degree dis and their ratio K as follows:

$$rad_i = \sqrt{\frac{1}{N}\sum_{n=1}^{N}(a_{in} - k_i)^2} \quad (1)$$

$$dis = \sqrt{\frac{1}{M}\sum_{i=1}^{M}(k_i - \bar{k_i})^2} \quad (2)$$

$$K = dis/rad_i \quad (3)$$

Where for a cluster with the number i, the corresponding cluster element set is a_{in}, and the core value is k_i, M is total number of clusters.

As rad_i reflects the tightness of each cluster and dis indicates the separation among different clusters, the value K can be used as an index of clustering validation. A higher K means higher concentration level of single clusters, and the larger distance between different clusters, in other words the effect of clustering is more significant **[40]**.

A control experiment was set here for the same period as ensemble forecast, which had a single member without perturbation and multi-scheme treatment. The result listed in table 1 below shows that compared to the single forecast, the ensemble average prediction has a higher correlation between forecasting error and weather types in weather classification.

Table 1. Cluster index K of control prediction (*K con*) and ensemble forecast (*K ens*).

Wind Field	*K con*	*K ens*
001	0.28	0.45
002	0.20	0.43
003	0.17	0.43
004	0.30	0.45
005	0.29	0.56
006	0.24	0.55
average	0.25	0.48

4.2. Ensemble forecast evaluation

To evaluate the ensemble forecasting, the sample came from 6 wind farms on the east coastal of China, from Sep. 2014 to Jan. 2015. In this section, we examined the effect of ensemble forecast with weather adapted correction with 28-52 h lead time.

4.2.1. Deterministic forecasting

When evaluating the deterministic forecasting of specific meteorological variables at a single site, root mean square error (RMSE) is one of the metrics that are commonly used. The variable reflects the overall level of prediction bias in the whole statistical sample. It can be calculated by the prediction bias e_i, which is the difference between forecast value v_i and observation value o_i, with a sample size of N.

$$rmse = \sqrt{\frac{1}{N}\sum_i^N e_i^2} \tag{4}$$

In discussion of ensemble prediction error, Hou et al. **[41]** made the following decomposition of RMSE with the reference work by Takacs **[42]**.

$$rmse^2 = mnbias^2 + sde^2 = mnbias^2 + sdbias^2 + disp^2 \tag{5}$$

Where:

$$mnbias = \overline{e_i} \tag{6}$$

$$sde = \sigma(e_i) \tag{7}$$

$$sdbias = \sigma(v_i) - \sigma(o_i) \tag{8}$$

$$disp = \sqrt{2\sigma(v_i) * \sigma(o_i) * (1 - r(v_i, o_i))} \tag{9}$$

$\sigma(v_i)$ and $\sigma(o_i)$ are standard deviations of prediction v_i and observation o_i, and $r(v_i, o_i)$ is the correlation coefficient between prediction and observation.

In this operation, rmse is divided into two parts: the mean bias of prediction *mnbias* and the standard deviation of prediction bias *sde*. Here the *mnbias* reflects a continuous overall deviation of prediction, while the *sde* indicates the fluctuation of forecast error around *mnbias*. Then *sde* is further decomposed into two parts: *sdbias* and *disp*. *Sdbias* is the difference between the standard deviation of prediction and observation, which refers to the bias of prediction with respect to the degree of wind speed fluctuation. *Sdbias* reflects the systematic error together with *mnbias*, which could be reduced by posterior statistical correction. Dispersion error *disp* represents the part of forecast error that is more difficult to be corrected, because this part of error comes from phase shifts instead of amplitude **[42]**.

In this test, a control prediction with a single member (SINGLE) was compared with ensemble average prediction (ENS). The original forecasts (OF) from the two forecasting systems were corrected by either the average bias correction method (AB) or the refined weather type adapted bias correction method (WAB). All these six predictions were evaluated by daily averaged RMSE. The results are listed in Table 2.

Table 2. Daily average RMSE (m/s) of six predictions, including original forecast (OF), average bias correction (AB), and weather adapted bias correction (WAB) outputs of the single member prediction (SINGLE) and the ensemble prediction (ENS).

Wind Field	SINGLE OF	SINGLE AB	SINGLE WAB	ENS OF	ENS AB	ENS WAB
001	2.68	2.29	2.21	2.71	2.09	1.86
002	3.41	2.87	2.75	2.83	2.14	1.90
003	3.22	2.80	2.74	2.70	2.09	1.96
004	1.53	1.53	1.63	2.42	1.95	1.84
005	2.94	2.56	2.45	3.01	2.35	2.17
006	2.47	2.29	2.28	2.23	1.95	1.78
average	2.71	2.39	2.34	2.65	2.10	1.92

According to the result, RMSE shows that ensemble forecast keeps a higher accuracy in both the original forecast and the corrected prediction. In addition, the average bias correction performs well in reducing the error of both ensemble forecast and single forecast, and weather adapted correction outperforms the traditional correction. Moreover, the improvement by weather type correction is more significant in ensemble prediction than in single forecast in the tested wind farms. Results of further analysis on RMSE of ensemble prediction are listed in tables followed.

Setting the original ensemble forecast as the reference forecast, we further defined the ratio of change that is made by two correction methods as follows for quantitative comparison:

$$K_{var} = 1 - \frac{var}{var_{ref}} \tag{10}$$

In the above equation var is the evaluation index of the forecast to be tested, and var_{ref} is the index of reference forecast. K_{var} indicates the capability of the correction method in reducing prediction error. K_{var} is positive only when prediction error is reduced. The higher K_{var} is, the better the correction method performs.

Table 3. Mean bias (m/s) and change rate (%) of original forecast (OF), average bias correction (AB), and weather adapted bias correction (WAB) outputs from the ensemble average forecast.

Wind Field	OF	AB	K_{AB}	WAB	K_{WAB}
001	2.40	0.68	0.72	0.64	0.73
002	2.47	0.81	0.67	0.78	0.68
003	2.33	0.77	0.67	0.75	0.68
004	1.95	0.68	0.65	0.62	0.68
005	2.57	0.85	0.67	0.80	0.69
006	1.67	0.51	0.70	0.46	0.72
average	2.23	0.72	0.68	0.68	0.70

Table 4. Standard deviation bias (m/s) and change rate (%) of three outputs of ensemble average forecast.

Wind Field	OF	AB	K_{AB}	WAB	K_{WAB}
001	0.77	0.89	**-0.16**	0.65	**0.16**
002	0.64	0.75	**-0.17**	0.48	**0.25**
003	0.46	0.55	**-0.18**	0.38	**0.18**
004	0.44	0.52	**-0.17**	0.42	**0.05**
005	0.75	0.85	**-0.14**	0.61	**0.18**
006	0.50	0.57	**-0.14**	0.31	**0.38**
average	0.59	0.69	**-0.16**	0.47	**0.20**

Table 5. Dispersion error (m/s) and change rate (%) of three outputs of ensemble forecast.

Wind Field	OF	AB	K_{AB}	WAB	K_{WAB}
001	2.13	2.34	-0.09	2.15	-0.01
002	2.26	2.43	-0.08	2.24	0.01
003	2.26	2.43	-0.07	2.31	-0.02
004	2.18	2.28	-0.05	2.19	-0.01
005	2.47	2.65	-0.07	2.51	-0.01
006	2.22	2.32	-0.04	2.17	0.02
average	2.25	2.41	-0.07	2.26	-0.00

From these three tables, we can compare two correction methods quantitatively by the *K* index for the three scenarios. The average bias correction makes a very huge improvement in the mean bias of prediction, but it doesn't help improve *sdbias* and *disp*, which even have a growth. By incorporating weather classification to the correction, the growth of *sdbias* caused by correction has been reduced, as highlighted in Table 4, and the *disp* index also shows improvements. Nonetheless, little influence is seen in *mnbias*.

4.2.2. Continuous Ranked Probability Skill (CRPS)

The continuous ranked probability skill (CRPS) is widely used in evaluation of ensemble systems. Compared with MAE and RMSE which evaluate error of a deterministic forecasting, CRPS considers the performance of all ensemble members. CRPS takes a measure to the difference between cumulative distribution function (CDF) of each member in ensemble forecast and the observation, and is usually used as an assessment of overall performance of ensemble prediction systems. It is computed by the formula

$$CRPS = \frac{1}{N}\sum_{i=1}^{N}\int_{-\infty}^{\infty}[F_i^f(x) - F_i^o(x)]^2 dx \tag{11}$$

where N is the volume of the sample, $F_i^f(x)$ is the CDF of the probabilistic forecast for the i-th value in the time series and $F_i^o(x)$ is the CDF of the corresponding observation. Thus we have:

$$F_i^f(x) = \int_{-\infty}^{x}\rho(y)dy \tag{12}$$

$$F_i^o(x) = H(x_i - x_i^a) \tag{13}$$

where

$$H(x) = \begin{cases} 0 & for\ x < 0 \\ 1 & for\ x \geq 0 \end{cases} \tag{14}$$

is known as the Heaviside function **[43, 44]**.

Here the CRPS of the original and corrected ensemble forecasts are given.

Table 6. CRPS of original (OF), AB and WAB corrected ensemble forecasts.

Wind Field	OF	AB	WAB
001	2.10	1.58	1.39
002	2.20	1.62	1.44
003	2.09	1.56	1.45
004	1.52	1.41	1.33
005	2.37	1.80	1.63
006	1.71	1.43	1.30
average	2.00	1.57	1.42

The CRPS score (CRPSS) is further used here to compare impacts of two correction methods, which is defined as follows **[44]**:

$$CRPSS = 1 - CRPS/CRPS_{OF} \tag{15}$$

The $CRPS$ is the index of corrected prediction, and $CRPS_{OF}$ is the original prediction as a reference. For the six wind farms in test, the $CRPSS$ of two correction methods are shown in Fig 3, which shows that WAB forecast has a stable and significant improvement against AB forecast ($CRPSS$ around 7% increment).

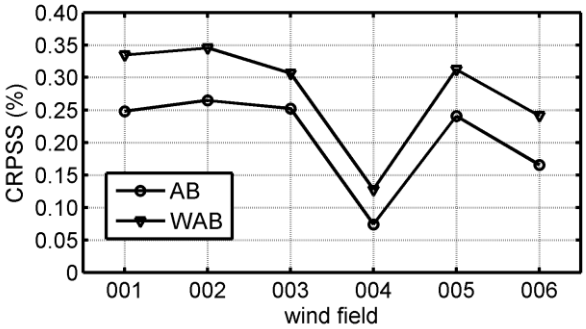

Figure 3. CRPS score in all tested wind farms, with a comparison between average bias correction (AB) and weather adapted bias correction (WAB).

4.2.3. Rank Histogram

As a method to directly reflect the consistency in statistical distributions between ensemble members' predictions and observation, rank histogram is widely used in evaluation of the reliability of ensemble prediction **[45,46]**. In this method, at each snap shot, the wind speed is divided into N+1 intervals by N forecast values of ensemble members, and the frequency that observation values fall in each interval is counted. In the ideal situation, the probability density distribution of ensemble members' prediction values should be consistent with that of observations, thus the observation should fall in each interval with the same probability, which means the rank histogram would have a flat distribution **[45,46]** (the black solid line in Fig 4). For the three predictions, data from all wind farms were used as the sample here. In order to directly compare the effect of correction methods, the mean values of absolute deviation (MAD) between the flat distribution and rank histograms of three different predictions are listed in Table 7 below.

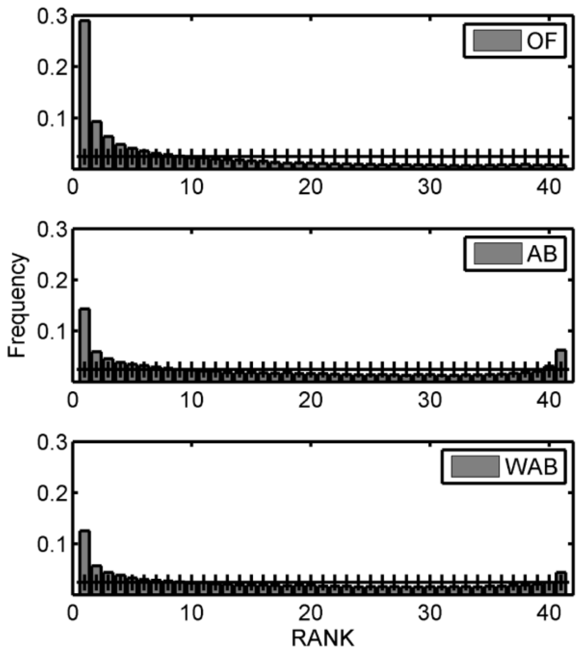

Figure 4. Rank histogram of ensemble forecasts, including original forecast (OF), and predictions from average bias correction (AB) and weather adapted bias correction (WAB). The black line with marks "+" is the ideal flat distribution.

Table 7. MAD values between the flat distribution and rank histograms.

	OF	AB	WAB
MAD	0.0212	0.0124	0.0100

In the upper panel of Figure 4, the rank histogram of original forecast (OF) has an "L" shaped distribution, which means the dominant part of ensemble members have larger prediction values than observation. The middle panel shows that the bias of prediction is effectively reduced after AB correction, producing a "U" shaped rank histogram. Nonetheless, some observations are still beyond the upper boundary of ensemble forecasts after correction, meaning that the predictions have been excessively corrected. The lower panel shows the histogram of predictions with a WAB correction. The excessive correction is mediated, and observations that fall below the lower boundary are further reduced. This improvement can also be observed from MAD values listed in Table 7.

5. Conclusion and discussion

In this research, an ensemble forecast system with 40 members was presented by adding initial random perturbation and multi-scheme to the GFS global forecasting fields. The forecasting system provided deterministic 70m wind speed predictions of single wind farms with a 15 min interval. This forecast results were further improved by developing a weather adapted error correction scheme, based upon the average bias correction method. The effect of correction methods were tested by ensemble forecasts from Sep. 2014 to Jan. 2015. Observations of 70m wind speed from wind towers were used as ground truth, with the same temporal resolution as the predictions.

In the evaluation of the weather classification, ensemble prediction outperformed single member forecast. This is because that compared with single member forecast, ensemble forecast comes from 40 different members, and tends to have a more stable performance under different weather types. This thus leads to a higher correlation between prediction error and weather type.

In the assessment of ensemble prediction, the deterministic prediction and the performance of all ensemble members were tested. The weather adapted correction outperformed conventional correction in both of the above two aspects.

In the AB correction method, an idealized assumption of bias accumulation was that the 6h averaged bias of prediction changes smoothly over time, while large fluctuations often occur in the practical forecast. These fluctuations would cause a deviation of bias estimation to subsequent prediction, and lead to an inadequate or excess correction. This type of bias in the correction is one of the main factors that cause an increase in *sdbias*.

By considering the impact of different weather types on prediction errors, the WAB correction method proposed in this research estimated and corrected prediction error fluctuations caused by the development of weather processes, and reduced the inadequate or excess correction caused by sudden severe changes of 6h average prediction bias. Therefore, compared with the AB correction method, the WAB correction method improved the prediction by reducing the bias in the standard deviation of prediction.

In Figure 5, four of all the 18 weather types are observed during the period of 7 days with different statistical typical errors, highlighted by different background colors. The 12th (red area, noted by WT=12 in Figure 5) weather type has a larger positive bias than the 1st (yellow area) type, which results in an overestimation of prediction bias after Oct. 15 through the bias estimation. The weather adapted correction method successfully reduced the excessive correction with respect to prediction (red line), and the WAB corrected prediction (blue line) shows an improvement compared with the AB prediction (green line).

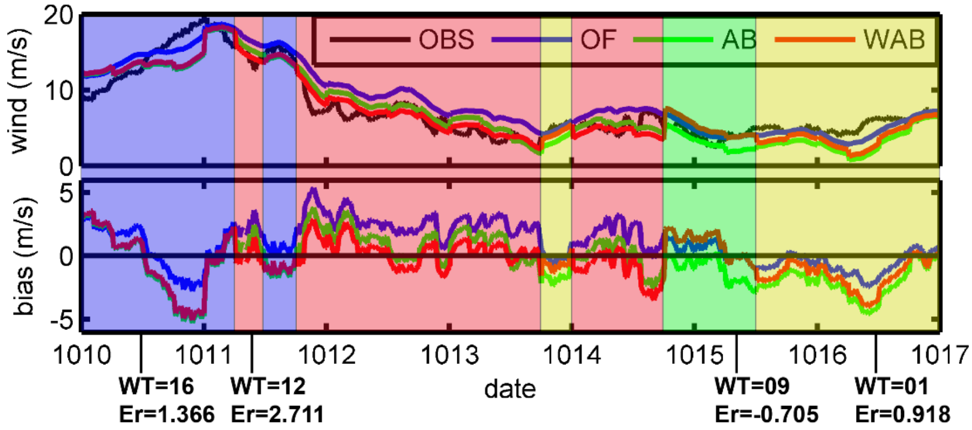

Figure 5. Original (OF, the blue solid line) and two corrected predictions (AB, the green line and WAB, the red line) outputs and observation data (real, the black), and corresponding forecast biases (solid lines in subplot below), with weather types in each period highlighted by background color. In lines below axis, WT shows the number of each period's weather type, and Er means the corresponding typical error of that weather type.

In this research, the refined weather adapted bias correction method is based on the assumption that there is a good correlation between local near-surface wind speed in wind farms and the weather types of this area. This also forms the basis of estimating the prediction errors through mesoscale weather fields in numerical weather predictions. If the local wind speed in the wind farm has a strong local property, and is rarely influenced by background weather field, the effect of correction would nonetheless deteriorate.

The sample wind farms are located in Jiangsu Province, the east coast of China, which is a flat area without complex terrain. Therefore the correlation between weather types and real wind speed is relatively clear. Similar performance of the newly developed correction method can be expected in offshore wind farms, while the effect may not be as satisfactory in mountainous areas.

Supplementary Materials: The following are available online at www.mdpi.com/link, Figure S1: title, Table S1: title, Video S1: title.

Acknowledgments: The study is partially supported by the research grants from the "Strategic Priority Research Program" of the Chinese Academy of Sciences (Grant No. XDA05040000), the National High Technology Research and Development Program (863 Major Project, Grant No. SQ2010AA1221583001) of China, and the National Natural Science Foundation of China (NSFC, Grant Numbers: 41175020 and 41375008).

Conflicts of Interest: The authors declare no conflict of interest.

Appendix A

Table A1. Number of ensemble members & schemes used in multi-scheme system.

MP	SFC	CU	PBL
14 Lin et al.	4 thermal diffusion	2 Kain-Fritsch,	1 YSU; 1 MYJ
	scheme	1 Betts-Miller,	1 YSU
		1 Grell-Devenyi	1 YSU
	4 unified Noah	2 Kain-Fritsch,	1 YSU; 1 MYJ
		1 Betts-Miller,	1 YSU
		1 Grell-Devenyi	1 YSU
	3 RUC	1 Kain-Fritsch,	1 YSU
		1 Betts-Miller,	

		1 Grell-Devenyi	
	3 Pleim-Xu	1 Kain-Fritsch, 1 Betts-Miller, 1 Grell-Devenyi	1 YSU
13 WSM 3-class simple ice scheme	3 thermal diffusion scheme	1 Kain-Fritsch, 1 Betts-Miller, 1 Grell-Devenyi	1 YSU
	4 unified Noah	2 Kain-Fritsch, 1 Betts-Miller, 1 Grell-Devenyi	1 YSU; 1 MYJ
	3 RUC	1 Kain-Fritsch, 1 Betts-Miller, 1 Grell-Devenyi	YSU
	3 Pleim-Xu	1 Kain-Fritsch, 1 Betts-Miller, 1 Grell-Devenyi	YSU
13 WSM 6-class scheme	3 thermal diffusion scheme	1 Kain-Fritsch, 1 Betts-Miller, 1 Grell-Devenyi	YSU
	4 unified Noah	2 Kain-Fritsch, 1 Betts-Miller, 1 Grell-Devenyi	1 YSU; 1 MYJ
	3 RUC	1 Kain-Fritsch, 1 Betts-Miller, 1 Grell-Devenyi	YSU
	3 Pleim-Xu	1 Kain-Fritsch, 1 Betts-Miller, 1 Grell-Devenyi	YSU

References

1. Jung J, Broadwater RP. Current status and future advances for wind speed and power forecasting. RENEW SUST ENERG REV. 2014;31:762-777.
2. Zhou W, Lou C, Li Z, Lu L, Yang H. Current status of research on optimum sizing of stand-alone hybrid solar-wind power generation systems. APPL ENERG. 2010;87:380-389.
3. Christensen JF. New control strategies for utilizing power system networks more effectively: The state of the art and the future trends based on a synthesis of the work in the cigre study committee 38. CONTROL ENG PRACT. 1998;6:1495-1510.
4. Al-Yahyai S, Charabi Y, Gastli A. Review of the use of Numerical Weather Prediction (NWP) Models for wind energy assessment. RENEW SUST ENERG REV. 2010;14:3192-3198.
5. Milligan MR, Miller AH, Chapman F. Estimating the Economic Value of Wind Forecasting to Utilities. Proceedings of Windpower. 1995.
6. Kalney E. Atmospheric modeling, data assimilation, and predictability: Cambridge University Press; 2003.

7. Negnevitsky M, Johnson P, Santoso S. Short term wind power forecasting using hybrid intelligent systems. 2007 IEEE Power Engineering Society General Meeting. 2007. p. 4.
8. Giebel G, Kariniotakis G, Brownsword R. The state-of-the-art in short term prediction of wind power from a danish perspective. J VIROL. 2003;82:9513-9524.
9. Ma L, Luan S, Jiang C, Liu H, Zhang Y. A review on the forecasting of wind speed and generated power. RENEW SUST ENERG REV. 2009;13:915-920.
10. Soman SS, Zareipour H, Malik O, Mandal P, "A review of wind power and wind speed forecasting methods with different time horizons," in North American Power Symposium, (2010), pp. 1-8.
11. Pinson P, Nielsen HA, Madsen H, Kariniotakis G. Skill forecasting from ensemble predictions of wind power. APPL ENERG. 2009;86:1326-1334.
12. Zhao E, Zhao J, Liu L, Su Z, An N. Hybrid Wind Speed Prediction Based on a Self-Adaptive ARIMAX Model with an Exogenous WRF Simulation. ENERGIES. 2016;9:7.
13. Bouzgou H, Benoudjit N. Multiple architecture system for wind speed prediction. APPL ENERG. 2011;88:2463-2471.
14. Sun W, Liu M, Liang Y. Wind Speed Forecasting Based on FEEMD and LSSVM Optimized by the Bat Algorithm. ENERGIES. 2015;8:6585-6607.
15. Alessandrini S, Sperati S, Pinson P. A comparison between the ECMWF and COSMO Ensemble Prediction Systems applied to short-term wind power forecasting on real data. APPL ENERG. 2013;107:271-280.
16. Traiteur JJ, Callicutt DJ, Smith M, Roy SB. A Short-Term Ensemble Wind Speed Forecasting System for Wind Power Applications. J APPL METEOROL CLIM. 2012;51:1763-1774.
17. Cui B, Toth Z, Zhu Y, Hou D. Bias Correction for Global Ensemble Forecast. WEATHER FORECAST. 2012;27:396-410.
18. Erdem E, Shi J. ARMA based approaches for forecasting the tuple of wind speed and direction. APPL ENERG. 2011;88:1405-1414.
19. Gallego C, Pinson P, Madsen H, Costa A, Cuerva A. Influence of local wind speed and direction on wind power dynamics - Application to offshore very short-term forecasting. APPL ENERG. 2011;88:4087-4096.
20. De Giorgi MG, Ficarella A, Tarantino M. Assessment of the benefits of numerical weather predictions in wind power forecasting based on statistical methods. ENERGY. 2011;36:3968-3978.
21. Cadenas E, Rivera W, Campos-Amezcua R, Heard C. Wind Speed Prediction Using a Univariate ARIMA Model and a Multivariate NARX Model. ENERGIES. 2016;9:109.
22. Barry RG, Perry AH. Synoptic climatology : methods and applications: Methuen; 1973.
23. Spinoni J, Szalai S, Szentimrey T, Lakatos M, Bihari Z, Nagy A, et al. Climate of the Carpathian Region in the period 1961-2010: climatologies and trends of 10 variables. INT J CLIMATOL. 2015;35:1322-1341.
24. Casado MJ, Pastor MA. Circulation types and winter precipitation in Spain. INT J CLIMATOL. 2016;36:2727-2742.
25. Burlando M. The synoptic-scale surface wind climate regimes of the Mediterranean Sea according to the cluster analysis of ERA-40 wind fields. THEOR APPL CLIMATOL. 2009;96:69-83.
26. B. Saavedra-Moreno ADLI. Surface wind speed reconstruction from synoptic pressure fields: Machine learning versus weather regimes classification techniques. WIND ENERGY. 2014.
27. Ramos AM, Pires AC, Sousa PM, Trigo RM. The use of circulation weather types to predict upwelling activity along the western Iberian Peninsula coast. CONT SHELF RES. 2013;69:38-51.
28. Addor N, Rohrer M, Furrer R, Seibert J. Propagation of biases in climate models from the synoptic to the

regional scale: Implications for bias adjustment. Journal of Geophysical Research: Atmospheres. 2016;121:2075-2089.

29. Skamarock WC, Klemp JB. A time-split nonhydrostatic atmospheric model for weather research and forecasting applications. J COMPUT PHYS. 2008;227:3465-3485.
30. SCHEMM CE, UNGER DA, FALLER AJ. Statistical Corrections To Numerical Predictions .3. MON WEATHER REV. 1981;109:96-109.
31. Huth R, Beck C, Philipp A, Demuzere M, Ustrnul Z, Cahynova M, et al. Classifications of Atmospheric Circulation Patterns Recent Advances and Applications. Annals of the New York Academy of Sciences2008. p. 105-152.
32. Zhang JP, Zhu T, Zhang QH, Li CC, Shu HL, Ying Y, et al. The impact of circulation patterns on regional transport pathways and air quality over Beijing and its surroundings. ATMOS CHEM PHYS. 2012;12:5031-5053.
33. Philipp A, Bartholy J, Beck C, Erpicum M, Esteban P, Fettweis X, et al. Cost733cat-A database of weather and circulation type classifications. PHYS CHEM EARTH. 2010;35:360-373.
34. Hoy A, Sepp M, Matschullat J. Large-scale atmospheric circulation forms and their impact on air temperature in Europe and northern Asia. THEOR APPL CLIMATOL. 2013;113:643-658.
35. Cahynova M, Huth R. Circulation vs. climatic changes over the Czech Republic: A comprehensive study based on the COST733 database of atmospheric circulation classifications. PHYS CHEM EARTH. 2010;35:422-428.
36. Demuzere M, Kassomenos P, Philipp A. The COST733 circulation type classification software: an example for surface ozone concentrations in Central Europe. THEOR APPL CLIMATOL. 2011;105:143-166.
37. Huth R. A circulation classification scheme applicable in GCM studies. THEOR APPL CLIMATOL. 2000;67:1-18.
38. Huth R. An intercomparison of computer-assisted circulation classification methods. INT J CLIMATOL. 1996;16:893-922.
39. Toreti A, Fioravanti G, Perconti W, Desiato F. Annual and seasonal precipitation over Italy from 1961 to 2006. INT J CLIMATOL. 2009;29:1976-1987.
40. CALINSKI T. A Dendrite Method For Cluster Analysis. BIOMETRICS. 1968;24:207.
41. Dingchen H, Kalnay E, Droegemeier KK. Objective verification of the SAMEX'98 ensemble forecasts. MON WEATHER REV. 2001;129:73-91.
42. TAKACS LL. A 2-step scheme for the advection equation with minimized dissipation and dispersion errors. MON WEATHER REV. 1985;113:1050-1065.
43. Hersbach H. Decomposition of the continuous ranked probability score for ensemble prediction systems. WEATHER FORECAST. 2000;15:559-570.
44. Alessandrini S, Delle Monache L, Sperati S, Nissen JN. A novel application of an analog ensemble for short-term wind power forecasting. RENEW ENERG. 2015;76:768-781.
45. Anderson JL. A method for producing and evaluating probabilistic forecasts from ensemble model integrations. J CLIMATE. 1996;9:1518-1530.
46. Hamill TM. Interpretation of rank histograms for verifying ensemble forecasts. MON WEATHER REV. 2001;129:550-560.